

# EPR spectroscopic characterization of an 'iron only' nitrogenase

## $S = 3/2$ spectrum of component 1 isolated from *Rhodobacter capsulatus*

Achim Müller<sup>a</sup>, Klaus Schneider<sup>a</sup>, Karlheinz Knüttel<sup>a</sup>, and Wilfred R. Hagen<sup>b</sup>

<sup>a</sup>Fakultät für Chemie, Lehrstuhl für Anorganische Chemie I, Universität Bielefeld, Bielefeld, Germany and <sup>b</sup>Department of Biochemistry, Agricultural University, Wageningen, The Netherlands

Received 26 March 1992

The alternative nitrogenase of *Rhodobacter capsulatus*, isolated from a *nifHDK* deletion mutant, has been purified to near homogeneity and identified as an 'iron only' nitrogenase. The dithionite-reduced component 1 ('FeFe protein') of this enzyme showed an EPR spectrum consisting of two components: a minor  $S = 1/2$  signal at  $g = 1.93$  and a very characteristic  $S = 3/2$  signal of near-stoichiometric intensity at  $g = 5.44$ . This resonance is very close to the highest possible  $g$  value ( $g = 5.46$ ) for the coinciding two intradoublet subspectra of an  $S = 3/2$  system of maximal rhombicity ( $E/D = 0.33$ ). The deviation from axial symmetry (increasing  $E/D$ ) correlates with the stability, activity and substrate selectivity of the different (Mo, V, Fe) nitrogenases.

Alternative nitrogenase; FeFe protein; Heterometal; Nitrogenase cofactor;  $S = 3/2$  EPR spectrum; *Rhodobacter capsulatus*

## 1. INTRODUCTION

It was like a paradigm change [1] when it became evident that three genetically distinct nitrogenase systems exist in bacteria [2–7], the 'classical' Mo-containing nitrogenase [8,9], a vanadium-containing one [2,3], and an 'iron only' nitrogenase [4,5,7] lacking both Mo and V. 'Iron only' nitrogenases have so far been isolated and biochemically characterized only in the case of *Azotobacter vinelandii* [4] and *Rhodobacter capsulatus* [7].

From the bioinorganic point of view it is of great importance to elucidate the influence of the heterometal center M (Mo, V, (Fe)) on the structure of the related protein and/or the corresponding metal cluster (FeMco with the composition  $\text{Fe}_x\text{MS}_y$  which may be present in different redox states [1]), on its electronic structure and especially on the selectivity for substrate reduction. The existence of nitrogenases with different heterometals within the catalytically active cluster center provides thus the opportunity for a better understanding of the  $\text{N}_2$  fixation mechanism by comparative biochemical and biophysical studies. Specific structural and spectroscopic properties by which the V- and the Fe-nitrogenase can be differentiated from each other are lacking until now. For the V-nitrogenase, isolated from *A. chroococcum* [2] and *A. vinelandii* [3,10,11] an  $S = 3/2$  EPR signal, assigned to the protein-bound cofactor, has

been detected which differs significantly from the characteristic  $S = 3/2$  signal of the MoFe protein. No EPR spectroscopic characterization of an  $S = 3/2$  spectrum has so far been presented for an 'Fe only' nitrogenase.

The 'FeFe protein' is component 1 of the Fe-nitrogenase from a *nifHDK* deletion mutant of *R. capsulatus* which is unable to synthesize the proteins of the conventional Mo-nitrogenase. In this note, we report an EPR spectrum of the 'FeFe protein' and correlate this spectrum with those of Mo- and V-nitrogenases [10,12,13]. Some comparable properties of the three nitrogenase systems including catalytical aspects are discussed, too.

## 2. MATERIALS AND METHODS

### 2.1. Bacterial strain and growth conditions

The organism used in this study was a *nifHDK*<sup>−</sup> strain generated from *R. capsulatus* B10S [7]. The cells were cultivated in 500-ml vacuum bottles under anaerobic, phototrophic conditions with serine (5 mM) as N-source and lactate (24 mM) as C-source as described [7]. The concentrations of some mineral salts in the nutrient solution were decreased as follows:  $\text{MgSO}_4 \cdot 7\text{H}_2\text{O}$  to 0.8 mM,  $\text{MnCl}_2 \cdot 4\text{H}_2\text{O}$  to 15  $\mu\text{M}$  and NaCl to 1.2 mM. The medium was additionally supplemented with EDTA (100  $\mu\text{M}$ ). The trace element solution containing Zn-, Cu-, Ni- and Co-chlorides [14] was omitted.

### 2.2. Harvest of cells and purification of component 1 of the Fe-nitrogenase

For enzyme purifications only freshly cultivated and harvested cells were used. Because *R. capsulatus* cells produced much slime during growth and sedimented poorly during centrifugation, before cell disruption the cultures were anaerobically harvested (under Ar in 4 mM  $\text{Na}_2\text{S}_2\text{O}_4$ ) by two centrifugation steps (in 500-ml bottles at  $14,000 \times g$  for 1 h and subsequently in 20-ml tubes at  $65,000 \times g$  for 1 h). The cell pellet obtained after the second centrifugation was resuspended in 50

Correspondence address: A. Müller, Lehrstuhl für Anorganische Chemie I, Universität Bielefeld, W-4800 Bielefeld, Germany. Fax: (49) (521) 106 6146.

mM Tris-HCl, pH 7.8, containing  $\text{Na}_2\text{S}_2\text{O}_4$  (8 mM) and roughly adjusted to a protein concentration of 25–30 mg/ml. To the cell suspension protease inhibitors ( $\alpha$ -N-benzoyl-L-arginine, 10 mM; phenylmethylsulfonyl fluoride, 2 mM) and superoxide dismutase from bovine erythrocytes (200  $\mu\text{g}/\text{ml}$ ) were added and the cells were then disrupted by passage through a French pressure cell. Further preparation steps and the purification of component 1 of the Fe-nitrogenase were performed as described previously [7].

### 2.3. Determinations of nitrogenase activity, protein and metal content

These were carried out as outlined in [7].

### 2.4. EPR measurement

EPR spectra were recorded on a Bruker ECS106 spectrometer (Bielefeld university) equipped with an ESP 1600 data system. Temperatures were maintained by liquid helium boil-off using an Oxford Instruments ESR 900 cryostat.

## 3. RESULTS AND DISCUSSION

In a preceding publication we described the alternative nitrogenase from *R. capsulatus*, in analogy to the 'nitrogenase-3' from *A. vinelandii* [4], as an instable and weakly active protein [7]. The component 1 of this enzyme was therefore found to be EPR-silent and in the form isolated generally unsuitable for physical studies. We have now been able to improve the conditions for derepression and stability of the alternative nitrogenase substantially. Of greatest importance have been several modifications in the composition of the growth medium (see section 2) and the use of highly concentrated cell suspensions (~30 mg protein/ml) supplemented with protease inhibitors and superoxide dismutase just before the breakage of the cells. (Details of the studies on stability and enzyme isolation will be published elsewhere.) We have thus obtained preparations of component 1 of about 95% purity and a specific activity of 42 nmol  $\text{C}_2\text{H}_2$  reduced/min/mg protein. By SDS-electrophoresis analyses we confirmed that this protein contains two types of large subunits near 60 kDa [7], but we also detected a band in SDS gels corresponding to an  $M_r$  ~15 kDa and this suggests an  $\alpha_2\beta_2\delta_2$  subunit composition as for the VFe proteins [6].

Metal analyses of the purest and most active component 1 preparation manifested that this protein contains only iron in relevant amounts. Compared to the previous preparation [7], the content of iron increased from 20 to 24 atoms/protein molecule, whereas the content of

other metals, including those discussed as potential heterometal atoms in nitrogenase (V, Re, W) decreased to negligible values (Table I). This was also true for Cu and particularly for Bi, in the preceding work interpreted as non-functional contaminants. Furthermore, by a semi-quantitative multielement analysis, comprising 69 elements, performed with an inductively coupled plasma mass spectrometer (ICP-MS), we have found that the concentration of all metals in the component 1 preparation was zero or nearly zero, except that of Fe and Zn ( $1.4 \pm 0.3$  atoms/molecule; Zn is known to bind unspecifically to the surface of many proteins). We conclude from these analyses that the alternative nitrogenase of *R. capsulatus* is, in fact, a heterometal — free 'iron only' nitrogenase.

With the purified component 1 (FeFe protein), reduced with dithionite, we obtained a low-temperature EPR spectrum (Fig. 1, 'preparation 1') which consists of two major components: a broad, asymmetric peak at  $g = 5.44$  and a feature with zero crossing at  $g = 1.93$ . Minor contaminations are detected at  $g = 4.4$ , 4.3 (adventitious ferric iron) and at  $g = 2.00$  (dithionite radical). The former signal was preparation dependent: the inset to Fig. 1 shows the respective part of the spectrum from a second less concentrated preparation ('preparation 2') in which the signal of the contaminating component was absent.

The spectrum (Fig. 1) was analyzed with the standard spin Hamiltonian for half-integer spin systems [15]:

$$H_s = \beta B \cdot g \cdot S + D[S_z^2 - S(S+1)/3] + E(S_x^2 - S_y^2) \quad (1)$$

For proteins and EPR at X-band frequencies the weak-field limit,  $D \gg g\beta B$ , is commonly a good assumption [16]. This implies that the sublevels of the spin multiplet arrange into  $(2S+1)/2$  well separated Kramers doublets. Each gives rise to an EPR subspectrum that can be described with a fictitious spin  $S' = 1/2$ , and with three effective  $g$  values which are a function of the ratio  $E/D$ , the 'rhombicity'. Assuming the real  $g$  tensor to be isotropic with the numerical value  $g = 2.00$ , we can calculate the effective  $g$  values and plot them as a function of  $E/D$ . The relevant 'rhombograms' have been calculated for  $S = 3/2$  through  $9/2$  [16–18]. We have recalculated the  $S = 3/2$  plot (Fig. 2) to make the point that the two panels for the two states with the spin wave functions  $|\pm 3/2\rangle$  and  $|\pm 1/2\rangle$  are symmetry-related in the sense that the extension of the lower panel along the horizontal rhombicity axis to  $E/D = \infty$  results in the (stretched) mirror image of the upper panel. From this observation it should be obvious that the two subspectra happen to be identical to each other for the specific case of full rhombicity, i.e.  $E/D = 1/3$ .

The observed effective  $g$  value of 5.44 is very close to the highest possible  $g$  value,  $g = 5.46$ , for the coinciding two intradoublet subspectra of an  $S = 3/2$  system of maximal rhombicity. Consistent with this interpretation

Table I

Metal content of component 1 of the alternative nitrogenase

Metal	Content in protein (atoms per molecule)	Metal	Content in protein (atoms per molecule)
V	0.02	Cu	0.18
Cr	0.09	Se	0
Fe	24	W	0.06
Co	< 0.01	Re	0.01
Ni	< 0.01	Bi	< 0.01
Zn	1.4	Mo	0.02

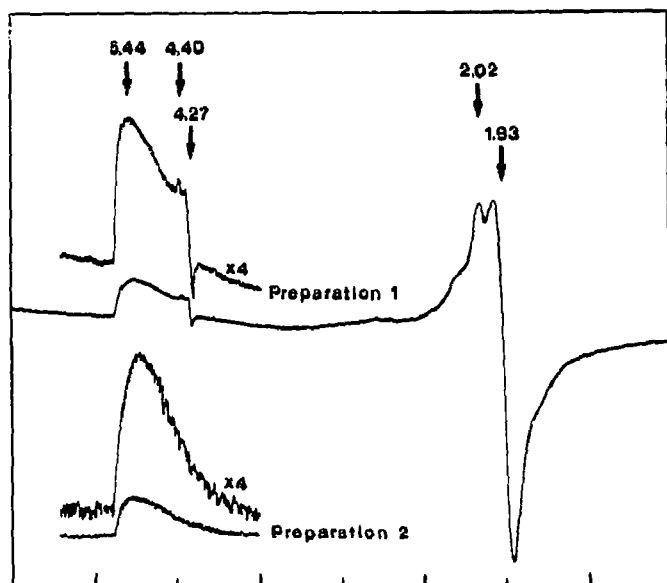


Fig. 1. EPR spectrum of the  $\text{Na}_2\text{S}_2\text{O}_4$ -reduced FeFe protein of the 'iron only' nitrogenase from *R. capsulatus*. Preparation 1: 24 mg protein/ml in 50 mM Tris buffer, pH 7.4, and 5 mM dithionite; preparation 2: 8.9 mg protein/ml in the same buffer. EPR conditions: microwave power, 20 mW; microwave frequency, 9.44 GHz; modulation amplitude, 1 mT. The spectra are base-line corrected with a frequency adjusted spectrum from a buffer-only sample.

we observed the shape of the feature at  $g = 5.44$  to be temperature-independent from 4 to 18 K, and the intensity to follow a simple Curie-law dependence.

Lowering the real  $g$  value from 2.00 to 1.99 reduces the effective  $g$  value to  $g = 5.44$ , two other effective  $g$  values are then expected at  $g = 1.99$  and 1.46. Inhomogeneous line broadening by a distribution in rhombicity gives rise to a form of  $g$  strain broadening [19]. Such a mechanism could easily cause the lines at the two other  $g$  values,  $g = 1.99$  and 1.46, to be broadened beyond detection. The two lines were previously detected as very broad features in the  $S = 3/2$  spectrum from a manganese complex; in this spectrum the low-field line is an order-of-magnitude sharper than the  $g = 5.44$  line described here [20]. A comparison of the two data sets indicates to us that the weak bump at  $\sim 270$  mT in the spectrum of the FeFe protein (see Fig. 1) might be the positive lobe of a very broad derivative feature around  $g = 1.99$ . Interestingly, Hales et al. have observed a comparable, very broad feature in the rapid adiabatic passage dispersion EPR of the *A. vinelandii* VFe protein ( $E/D = 0.26$ ), however, these authors chose to assign this feature to an — otherwise unspecified — third paramagnetic site [11].

In view of the previous it is likely that the signal at  $g = 1.93$  does not represent a part of the  $S = 3/2$  system, but is rather due to a separate  $S = 1/2$  system. This signal 'saturated' at high microwave power and was strongest at 9–12 K. As the intensity varied from prep-

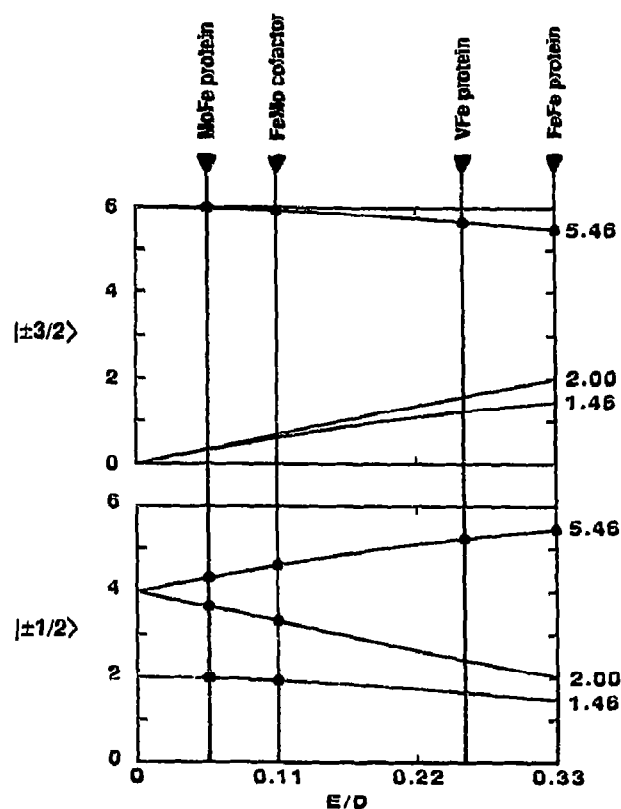


Fig. 2.  $S = 3/2$  rhombogram (for the two low-energy Kramers doublets  $|\pm 3/2\rangle$  and  $|\pm 1/2\rangle$ ) giving the relation between effective  $g$  values and rhombicity,  $E/D$ , in the weak-field limit and assuming an isotropic real  $g$  value of 2.00. The vertical bars represent the approximate rhombicities and  $g$  values for the different types of nitrogenase component 1 and for the isolated cofactor, where we have ignored reported small deviations from  $g_{\text{real}} = 2.00$ . Dots (•) indicate experimentally observed  $g$  values. The resonance peak at  $g = 6.0$  of the FeMoco in the protein-bound state has so far only been detected in the case of the MoFe protein from *Clostridium pasteurianum* [28].

aration to preparation, its origin is still uncertain. A very similar  $S = 1/2$  signal has been described for the V-containing nitrogenases [2,3] and has recently been noted also for the nitrogenase-3 system of *A. vinelandii* [21].

We are left with a very characteristically shaped  $g = 5.44$  peak with a broad tail at high field and a cut-off at low field. This can also be explained within the framework of an  $S = 3/2$  spin system of distributed rhombicity. The effective  $g$  value can be spread out, however, to the low-field side not beyond the theoretical maximum of  $g = 6$  (cf. Fig. 2). An attempt was made also to fit the  $g = 5.44$  spectrum to each of the patterns predicted for the spins  $S = 5/2$ ,  $7/2$ , and  $9/2$  [16–18], however, only an  $S = 3/2$  system is consistent with the spectrum in Fig. 1. Since for maximum rhombicity ( $E/D = 1/3$ ) both observed subspectra are identical, we can quantify without a Boltzmann correction within the spin multiplet. Using the  $S = 3/2$  signal from a *A. vinelandii* MoFe protein [12] preparation (specific activity

1800 nmol  $C_2H_2$  reduced/min/mg protein) as the external standard and referring to the  $g = 4.3$  peak that corresponds to the  $g = 5.44$  peak of the FeFe protein, we found approximately two (1.8)  $S = 3/2$  spin systems per 258 kDa hexameric FeFe protein.

Whereas the described  $g = 5.44$  peak represents, in agreement with the theoretical calculations, the only 'visible' resonance of this  $S = 3/2$  spectrum, the VFe protein from *A. vinelandii* showed, due to a less pronounced rhombicity, inflections at  $g = 5.8$  and  $5.4$  resulting from the superposition of two subspectra (see also Fig. 2) distinguishable by a different temperature dependence [10]. The published  $S = 3/2$  spectrum of the VFe protein from *A. chroococcum* is more complex and difficult to analyze ( $g$  values at 5.60, 4.35, 3.77) as it appears to arise from a mixture of cofactor species [22].

A vertical bar at  $E/D = 0.33$  (Fig. 2) indicates the rhombicity and effective  $g$  values for the *R. capsulatus* FeFe protein. The literature data for the MoFe protein from *A. vinelandii* ( $E/D = 0.055$ ) [12], the isolated FeMo cofactor ( $E/D = 0.11$ ) [13], and *A. vinelandii* VFe protein ( $E/D = 0.26$ ) [10] fit nicely into the plot. Apparently, modulation of the cofactor, by changing the heterometal and/or the environment, can cause the symmetry felt by the  $S = 3/2$  spin to vary almost over the entire theoretically possible range.

The deviation from axial (roughly spherical) symmetry of component 1 (increasing rhombicity) correlates with the stability, activity and substrate selectivity of the different nitrogenases:

MoFe protein > VFe protein >> FeFe protein

In this row, from left to right, (i) the stability and (ii) the specific activity (with  $N_2$  and  $C_2H_2$  as substrate) decreases, (iii) the ratio of  $C_2H_6/C_2H_4$  formation upon  $C_2H_2$  reduction increases (note that there is only one conventional Mo-nitrogenase system known — the one from *Xanthobacter autotrophicus* — that produces  $C_2H_6$  from  $C_2H_2$  (K. Schneider, unpublished results)) and the ratio of competitive  $H^+/C_2H_2$  ( $H^+/N_2$ ) reduction rates increases as well (for review, see [6]). Because of these obvious correlations we tentatively assign the  $S = 3/2$  spectrum of the FeFe protein, in analogy to the assignment of the corresponding signals of Mo- and V-nitrogenases, to a comparable M-cluster ('FeFeco').

The results presented here, together with the facts that  $C_2H_6$  formation is also observed after site directed mutation of the MoFe proteins causing a change in the environment of the cofactor [23] and that Mo is at least electronically not strongly coupled with the  $Fe_4S_4$  cluster fragment [24,25], support the hypothesis, that the Mo center is not directly involved in substrate ( $N_2$ ) binding but that it is rather responsible for producing a 'more stable' and catalytically more effective cluster shape. Assuming now that this is the real function of the heterometal, from the catalytic and stability properties

of the different nitrogenases it can be concluded that this is best fulfilled by Mo.

Interesting related problems are the influence of the apoprotein on the  $E/D$  ratio (compare values of the protein-bound and isolated FeMoco), the probable influence of the cluster shape on the affinity towards substrates and their reaction products during enzyme turnover and its influence on the formation of  $C_2H_6$  from  $C_2H_2$ , and finally, the evolution of the three nitrogenase systems (cf. different abundance and availability (solubility) of molybdenum (abundant as insoluble  $MoS_2$ ), vanadium (insoluble  $VOOH$ ) and iron (soluble  $Fe^{2+}$ ) on the precambrian earth [26]) and their possible different roles in substrate (e.g.  $CN^-$ ) [27] reductions in the early stages of evolution.

**Acknowledgements:** We thank S. Selsemeier for technical assistance and Dr. W. Klipp for providing the *nifHDK* mutant of *R. capsulatus*. This work was supported by the Deutsche Forschungsgemeinschaft (DFG) and the Fonds de Chimischen Industrie. We also thank the Bundesministerium für Forschung und Technologie (BMFT) for providing us an ICP-mass spectrometer.

## REFERENCES

- [1] Burgess, B.K. (1990) Chem. Rev. 90, 1377–1406.
- [2] Eady, R.R., Robson, R.L., Richardson, T.H., Miller, R.W. and Hawkins, M. (1987) Biochem. J. 244, 197–207.
- [3] Hales, B.J., Case, E.E., Morningstar, J.E., Dzeda, M.F. and Mutterer, L.A. (1986) Biochemistry 25, 7251–7255.
- [4] Chisnell, J.R., Premakumar, R. and Bishop, P.E. (1988) J. Bacteriol. 170, 27–33.
- [5] Cammack, R. (1988) Nature 333, 595–596.
- [6] Pau, R.N. (1991) in: Biology and Biochemistry of Nitrogen Fixation (M.J. Dilworth and A.R. Glenn, Eds.), Elsevier, Amsterdam, pp. 37–57.
- [7] Schneider, K., Müller, A., Schramm, U. and Klipp, W. (1991) Eur. J. Biochem. 195, 653–661.
- [8] Gresshoff, P.M., Roth, E., Stacey, G. and Newton, W.E. (1990) in: Nitrogen Fixation: Achievements and Objectives, Chapman and Hall, New York/London.
- [9] Müller, A. and Newton, W.E. (1983) Nitrogen Fixation. The Chemical-Biochemical-Genetic Interface, Plenum Press, New York/London.
- [10] Morningstar, J.E. and Hales, B.J. (1987) J. Am. Chem. Soc. 109, 6854–6855.
- [11] Hales, B.J., True, A.E. and Hoffmann, B.M. (1989) J. Am. Chem. Soc. 111, 8519–8520.
- [12] Münck, E., Rhodes, H., Orme-Johnson, W.H., Davis, L.C., Brill, W.J. and Shah, V.K. (1975) Biochim. Biophys. Acta 400, 32–53.
- [13] Rawlings, J., Shah, V.K., Chisnell, J.R., Brill, W.J., Zimmermann, R., Münck, E. and Orme-Johnson, W.H. (1978) J. Biol. Chem. 253, 1001–1004.
- [14] Soefert, E. and Pfennig, N. (1980) Arch. Microbiol. 125, 73–77.
- [15] Abragam, A. and Bleaney, B. (1970) Electron Paramagnetic Resonance of Transition Ions, Clarendon Press, Oxford.
- [16] Hagen, W.R., Wassink, H., Eady, R.R., Smith, B.E. and Haaker, H. (1987) Eur. J. Biochem. 169, 457–465.
- [17] Moura, I., Macedo, A. and Moura, J.J.G. (1989) in: Advanced EPR: Applications in Biology and Biochemistry (A.J. Hoff, Ed), Elsevier, Amsterdam, pp. 813–838.
- [18] Pierik, A.J. and Hagen, W.R. (1991) Eur. J. Biochem. 195, 505–516.
- [19] Hagen, W.R. (1981) J. Magn. Reson. 44, 447–469.

- [20] Hoffmann, B.M., Weschler, C.J. and Basolo, F. (1976) *J. Am. Chem. Soc.* 90, 5473-5482.
- [21] Scorson, K.A., Moore, V.G. and Hales, B.J. in: *Nitrogen Fixation: Achievements and Objectives* (P.M. Gresshoff, E. Roth, G. Stacey and W.E. Newton, Eds.), Chapman and Hall, New York/London, p. 837.
- [22] Eady, R.R., Pau, R., Lowe, D.J. and Luque, F.J. (1990) in: *Nitrogen Fixation: Achievements and Objectives* (P.M. Gresshoff, E. Roth, G. Stacey and W.E. Newton, Eds.), Chapman and Hall, New York/London, pp. 125-133.
- [23] Scott, D.J., May, H.D., Newton, W.E., Brigle, K.E. and Dean, D.R. (1990) *Nature* 343, 188-190.
- [24] Smith, B.E. (1983) in: *Nitrogen Fixation. The Chemical-Biochemical-Genetic Interface* (A. Müller, and W.E. Newton, Eds.), Plenum Press, New York/London, pp. 23-62.
- [25] Venters, R.A., Nelson, M.J., McLean, P.A., True, A.E., Levy, M.A., Hoffmann, B.M. and Orma-Johnson, W.H. (1986) *J. Am. Chem. Soc.* 108, 3487-3498.
- [26] Erskamp, J. and Müller, A. (1990) *Chemie in unserer Zeit* 6, 267-279.
- [27] Postgate, J.R. (1974) in: *Evolution in the Microbial World*, 24<sup>th</sup> Symposium of the Society for General Microbiology, Cambridge University Press, Cambridge.
- [28] George, G.N., Bare, R.E., Jin, H., Stiefel, E.I. and Prince, R.C. (1989) *Biochem. J.* 262, 349-352.